Optimal Design and Control of Electric Vehicle Transmissions

van den Hurk, J.L.J.

Award date:
2021

Optimal Design and Control of Electric Vehicle Transmissions

Juriaan van den Hurk
Supervisor: Dr. Ir. Mauro Salazar

***Abstract*—This thesis presents models and optimization methods to jointly optimize the design and control of the drivetrain of electric vehicles. First, considering the motor power to be given, we identify a convex speed-dependent motor model. Second, we devise effective algorithms to determine the optimal design and control of fixed-gear transmissions, multiple-gear transmissions and continuously variable transmissions. Finally, we present a case study for a compact family vehicle drive-cycle. We validate our approach with a quadratic motor model and globally optimal results obtained with mixed-integer convex programming. Our results show that by using a 2-speed transmission, the energy consumption of an electric vehicle can be reduced by 3% and 2.5% compared to a fixed-gear transmission and a continuously variable transmission, respectively.**

I. Introduction

In the global shift away from fossil fuels, the transport sector is transitioning towards zero-emission alternatives for the traditional internal combustion engine (ICE). One of these alternatives are electric vehicles (EVs). EVs have a great potential to replace ICE vehicles, with sales substantially increasing every year around the world [1] [2]. In this context, the continuous development of EV technologies is crucial in ensuring its competitiveness [3]. One of the technological challenges is to increase the energy efficiency of the EVs. This has several benefits: A major barrier for the adoption of battery electric vehicles (BEVs) is the concern about their range [4] [5]; Increasing energy efficiency will improve the range of BEVs and therefore, will contribute towards their adoption. Furthermore, increasing energy efficiency allows for downsizing the battery and the motor, hence decreasing the total cost of the vehicle, which will make BEVs more attractive to the public [6].

Improving the energy consumption of EVs is a major technological challenge. Different techniques to increase the efficiency of different components have been implemented already. The shape of the body has been made more aerodynamic to reduce drag, the mass of various components has been reduced, the recuperation of energy via regenerative braking has been introduced and the powertrain has been rendered more efficient through intelligent energy management strategies. To increase the energy efficiency of BEVs, optimal design and control of a BEV powertrain can be used. [1]. Against this background, this project will focus on the optimization of the design and control of the EV drivetrain shown in Fig. 1. Furthermore, the possibility of sizing the motor will be taken into consideration. The optimization of the control of the drivetrain and the design of the transmission

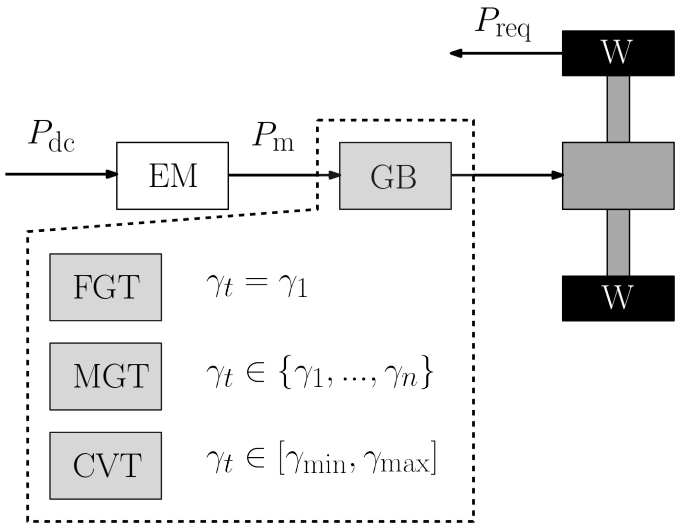

Fig. 1. Schematic representation of the modeled vehicle. It exists of an electric motor (EM), a gearbox (GB) and the wheels (W). The arrows indicate the power flow between the components.

will increase energy efficiency, improving the range of the EV. The downsizing of the the motor will decrease the cost of the EV. Finally, a comparison will be made between a multi-gear transmission (MGT), a continuously variable transmission (CVT) and a fixed-gear transmission (FGT). One of the challenges of finding the optimal gear ratios and shifting strategy is the combinatorial nature of the problem. The optimal shifting patterns change with the gear ratios themselves. Furthermore, the motor size can be varied with more efficient gear ratios and shifting patterns. Therefore, the problem can be split into two parts: (i) control of the gear shift command and the power that needs to be supplied, and (ii) design of the gear ratios and the drivetrains' component size.

Literature review: A number of strategies have been used for the control of electric vehicles. In [7] a genetic algorithm is used to come to an optimal shifting pattern for an electric vehicle. Convex optimization has been used to find the gear selection and power distribution for a hybrid electric vehicle (HEV), leveraging Pontryagin's principle in [8]. A combination of a method to solve non-convex problems and convex optimization is also possible. The combination of dynamic programming and Pontryagin's principle has been applied to find the optimal control of the gearshift command in HEVs [9]. Similarly, a combination of convex optimization

and dynamic programming was employed in [10] to find the optimal gearshift command, engine on/off state and power split for an HEV. Convex optimization was also used in an iterative method to come to a fast algorithm to find the optimal energy management strategy for HEVs [11]. In [12], convex optimization is used to find the optimal power split control for an HEV. However, none of these techniques involve the optimization of the design of the transmission.

Many approaches have been applied for the design of EV drivetrain components. The authors of [13] propose a method leveraging convex optimization to simultaneously find an optimal battery size and an optimal energy management strategy for a HEV. In [14], the transmission design and control design have been optimized simultaneously. This was done for an FGT gearbox and a CVT. In [15], mixed integer nonlinear programming was used to find the optimal gear ratios for a multi-speed gearbox. An optimal control strategy to change gears was included in this research. The method proposed in [16] finds the optimal gear ratios for varying gear shift maps. This way the optimal combination of gear shift maps and gear ratios is found. This is done by a brute force algorithm which calculates all the different combinations to find the optimum. Building on the method of [16] to find the optimal gear ratios, the authors of [17] propose a method based on dynamic programming to find the optimal gear shift commands for the ratios found using the methods in [16]. This way, the combinatorial problem of finding the gear ratios and the gear shift commands has been solved. The methods in [18] include the design of new motors, the optimization of gear ratios and the search for the most advantageous drivetrain layout. Whilst the methods in [14] [15] [18] and the combination of the methods in [16] and [17] all in some form solve the combinatorial problem of finding the optimal gear ratios and control strategy, they involve nonlinear optimization methods and brute force algorithms that result in high computation times.

Perhaps closest to our work in spirit are the following contributions: First, convex optimization is used to find the optimal control strategies for a race car to achieve minimal lap times in [19]. Furthermore, the design of a single-speed transmission and the control of a CVT are optimized. In contrast to the methods for transmission design mentioned earlier, the use of convex optimization ensures computational efficiency and global optimality guarantees. Even though the optimization is in terms of lap time, the used vehicle model and optimization techniques are still highly relevant for the purposes of this project.

Second, a method to jointly design the gearbox and find an optimal control algorithm was proposed in [20]. Convex optimization was used to arrive at a computationally efficient result. This was achieved by carefully approximating and relaxing the constraints on the vehicle model. The method provided similar results to a particle swarm optimization approach, with only a fraction of the computational cost. The method provided an increase in efficiency for a heavy-duty truck of 1-10 %. Furthermore, the electric motor size could be reduced by 20-50 %. In both [19] and [20] the design and control of the transmission and drivetrain have been optimized in an integrated fashion. Furthermore, the optimization was effected in a computationally efficient manner, explicitly accounting for the combinatorial nature of the problem and with global optimality guarantees. However, the methods only include a CVT and an FGT. To the best of the authors' knowledge, a method to jointly optimize the design and control of an MGT in a computationally efficient manner is not available yet.

Statement of Contributions: This project will add to the methods and results obtained in [20] by implementing a method to jointly optimize the gear design and the gear strategy for an FGT, MGT and CVT. In contrast to the methods in [16], [17], [15] and [18], particular optimization techniques will be applied to attain a computationally efficient algorithm. A combination of dynamic programming and convex optimization will be employed and the optimization will be done offline over a known drive cycle. This way, the drive cycle can be discretized and quasi-static vehicle component models can be used. A comparison will be made between FGTs, MGTs and CVTs in terms of energy efficiency. Finally, the methods will be validated by checking the results with nonlinear simulations and comparing them to globally optimal results obtained with mixed-integer quadratic programming (MIQP).

Thesis Structure: The remainder of this thesis will be structured as follows: First, a model of an EV will be presented, including a convex motor model in Section II. Furthermore, methods to find the optimal gear designs and strategies for a CVT, FGT and MGT, respectively and a way to size the EM will be presented in Section II as well. In Section III, the results are presented for all three types of transmissions and a method for validation is applied. Finally, the conclusions are presented in Section IV.

II. Methodology

In this section, we present the methodology in the following order: First, a model of the EV and its transmission will be introduced. Second, we model the electric motor in Section II-C. Third, we present methods for the optimal design and control of the CVT, FGT and MGT, respectively in Sections II-D, II-E and II-F. Finally, a method to size the electric motor is described in Section II-G. For the sake of simplicity we will ignore time-dependency as well as power-dependency whenever it is clear from the context.

A. Vehicle and Transmission

A quasi-static modeling approach is used as described in [21]. A schematic representation of the vehicle can be seen in Fig. 1. For a given driving cycle, existing of a velocity trajectory $v(t)$, an acceleration trajectory $a(t)$ and a road grade trajectory $\alpha(t)$, the required power can be calculated as

$$\begin{aligned} P_{\mathrm{req}} =& m_{\mathrm{v}} \cdot (c_{\mathrm{r}} \cdot g \cdot \cos(\alpha) + g \cdot \sin(\alpha) + a) \cdot v \\ &+ \frac{1}{2} \cdot \rho \cdot c_{\mathrm{d}} \cdot A_{\mathrm{f}} \cdot v^3, \end{aligned} \tag{1}$$

where m_v is the total mass of the vehicle, c_r is the rolling friction coefficient, g is the gravitational acceleration, ρ is the air density, c_d is the air drag coefficient and A_f is the frontal area of the vehicle.

The transmission efficiencies differ for the FGT, MGT and CVT and are assumed to be constant. The power that is required from the motor is therefore different for these types of transmission. The motor power that is required to follow the drive cycle trajectory is

$$P_\mathrm{m} = \begin{cases} P_\mathrm{req} \cdot \eta_\mathrm{fgt}^{-\mathrm{sign}(P_\mathrm{req})} & \text{if FGT} \\ P_\mathrm{req} \cdot \eta_\mathrm{mgt}^{-\mathrm{sign}(P_\mathrm{req})} & \text{if MGT} \\ P_\mathrm{req} \cdot \eta_\mathrm{cvt}^{-\mathrm{sign}(P_\mathrm{req})} & \text{if CVT} \end{cases}, \tag{2}$$

where η_fgt, η_mgt and η_cvt are the efficiencies of the FGT, MGT and CVT, respectively and are considered as given.

Therefore, the operating point of the electric motor is solely determined by the transmission. The rotational motor speed ω_m is related to the speed through the transmission ratio γ via

$$\omega_\mathrm{m} = \gamma \cdot \frac{v}{r_\mathrm{w}}, \tag{3}$$

where, r_w is the wheel radius. The transmission ratio is subject to optimization and varies for different types of transmissions. For an FGT, the transmission is fixed. For an MGT, the transmission can be varied between fixed values. For a CVT, the transmission can operate at any value. These different cases are described by

$$\gamma(t) \begin{cases} = \gamma_1 & \text{if FGT} \\ \in \{\gamma_1, ..., \gamma_{n_\mathrm{gears}}\} & \text{if MGT} \\ \in [\gamma_\mathrm{min}, \gamma_\mathrm{max}] & \text{if CVT} \end{cases}, \tag{4}$$

where $\gamma_1, ..., \gamma_{n_\mathrm{gears}}$ are fixed gear ratios of the FGT and MGT and n is the number of gears in the MGT, whilst γ_min and γ_max are the gear ratios that determine the range of the CVT.

In order to be able to start driving uphill on a slope of α_0, we must satisfy

$$m_\mathrm{v} \cdot g \cdot \sin(\alpha_0) \cdot r_\mathrm{w} \leq T_\mathrm{m,max} \cdot \begin{cases} \eta_\mathrm{fgt} \cdot \gamma_1 & \text{if FGT} \\ \eta_\mathrm{mgt} \cdot \gamma_1 & \text{if MGT} \\ \eta_\mathrm{cvt} \cdot \gamma_\mathrm{max} & \text{if CVT} \end{cases}. \tag{5}$$

B. Vehicle Mass

The mass of the vehicle varies for different transmission types. The total mass of the vehicle m_v is the sum of a base weight m_0, the weight of the gearbox m_g and the weight of the motor m_m, yielding

$$m_\mathrm{v} = m_0 + m_\mathrm{g} + m_\mathrm{m}. \tag{6}$$

Similarly to [20], the motor mass m_m is modeled linear in relation to the maximum motor power $P_\mathrm{m,max}$ as

$$m_\mathrm{m} = \rho_\mathrm{m} \cdot P_\mathrm{m,max}, \tag{7}$$

where ρ_m represents the specific mass of the motor. The mass of the gearbox is modeled linearly with the number of gears as

$$m_\mathrm{g} = \begin{cases} m_\mathrm{g,0} + m_\mathrm{gw} & \text{if FGT} \\ m_\mathrm{g,0} + m_\mathrm{gw} \cdot n_\mathrm{gears} & \text{if MGT} \\ m_\mathrm{cvt} & \text{if CVT} \end{cases}, \tag{8}$$

where $m_\mathrm{g,0}$ is the base mass for an FGT and an MGT, m_gw is the added mass per gear, n_gears is the number of gears and m_cvt is the mass of a CVT.

C. Motor Model

While previous loss-based models, such as the quadratic model from [19], are based on the speed of the EM, for the purposes of this project we use a different approach. The power loss will be modeled based on speed and motor power. This can be done because a quasi-static approach is used. For each specific motor power, the power loss is determined with a function of the motor speed ω_m via

$$P_\mathrm{m,loss} = \frac{p_0(P_\mathrm{m})}{\omega_\mathrm{m}} + p_1(P_\mathrm{m}) + p_2(P_\mathrm{m}) \cdot \omega_\mathrm{m}, \tag{9}$$

where the coefficients p_0, p_1 and p_2 are dependent on the motor power P_m. In this case, the model consists of a fractional term, a constant and a linear term. In order to ensure convexity on the positive domain,

$$p_0(P_\mathrm{m}) \geq 0 \;\forall\; P_\mathrm{m} \tag{10}$$

and

$$p_2(P_\mathrm{m}) \geq 0 \;\forall\; P_\mathrm{m} \tag{11}$$

must be applied.

Another constraint is applied in order to keep the efficiency from rising too much at the point where the power loss is lowest as

$$P_\mathrm{m,loss} \geq \min(\overline{P}_\mathrm{m,loss}), \tag{12}$$

where $\overline{P}_\mathrm{m,loss}$ is the power loss from the measured EM data. The coefficients p_0, p_1 and p_2 have to be found for each power level. This can be accomplished using optimization software. The result is a collection of coefficients p_0, p_1 and p_2 that is stored in a matrix. Each set of coefficients corresponds to a certain motor power. The corresponding powers are stored in a vector P_vector. In applying the model above, one can use interpolation to obtain the coefficients and then determine the power loss according to (9).

In order to show the logic behind this method of modeling, we show the power loss and the fitted power loss resulting from (9) to (12) in Fig. 2 for different power levels. One can see how the fitted model follows the trend of the measured model quite neatly. Furthermore, the choice of the model with the fractional term becomes evident, as well as the need for constraint. (12). This approach to EM modeling can also be used in different ways, such as choosing a quadratic model.

The input power P_dc can be determined as

$$P_\mathrm{dc} = P_\mathrm{m} + P_\mathrm{m,loss}. \tag{13}$$

The motor operating point is bound by three factors: the maximum power, the maximum torque and the maximum

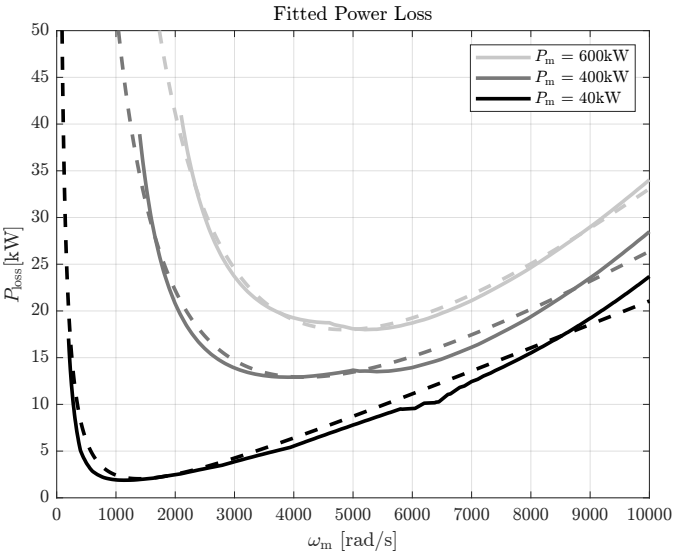

Fig. 2. The power loss from motor data and the fitted power loss from the model. The solid lines indicate the real values and the dashed lines indicate the fit.

motor speed. This leads to the following constraints: the constraint limiting the motor speed described by

$$\omega_{\mathrm{m}} \in [0, \omega_{\mathrm{m,max}}], \tag{14}$$

where $\omega_{\mathrm{m,max}}$ is the maximum motor speed; the constraint limiting the torque described by

$$P_{\mathrm{m}} \in [-T_{\mathrm{m,max}}, T_{\mathrm{m,max}}] \cdot \omega_{\mathrm{m}}, \tag{15}$$

where $T_{\mathrm{m,max}}$ is the maximum torque; the maximum power constraint can be described by an affine function

$$P_{\mathrm{m}} \in [-c_{\mathrm{m1}} \cdot \omega_m - c_{\mathrm{m2}}, c_{\mathrm{m1}} \cdot \omega_{\mathrm{m}} + c_{\mathrm{m2}}], \tag{16}$$

where $c_{\mathrm{m1}} \leq 0$ and $c_{\mathrm{m2}} \geq 0$ are constants.

The model described by (9) - (16) is fitted to the measured motor map of Fig. 3. The resulting normalized root mean square error (RMSE) is 0.26 %. The efficiency map resulting from the fitted model is shown in Fig. 4. If the efficiency map from the model is compared to the measured motor map, one can see that the trends of the EM are captured quite well in the fitted model.

Discussion: An issue that has to be addressed regarding this motor model is its validity at low motor speeds. The fractional term in (9) causes the power loss to go to infinity when the motor speed goes to zero. To remedy this, the coefficients p_0 and p_2 are set to 0 when the motor speed is very low. Whilst this is a drawback of this particular model, it is still a valiant option due to its accuracy and convergence speed in all other areas. For future research purposes, the possibility of moving the asymptote of the model by introducing a constant ω_o can be examined. The model then becomes

$$P_{\mathrm{m,loss}} = \frac{p_0}{\omega_{\mathrm{m}} + \omega_o} + p_1 + p_2 \cdot \omega_{\mathrm{m}}.$$

However, the asymptote can not be moved when the methods in Sections II-D, II-E and II-F are used.

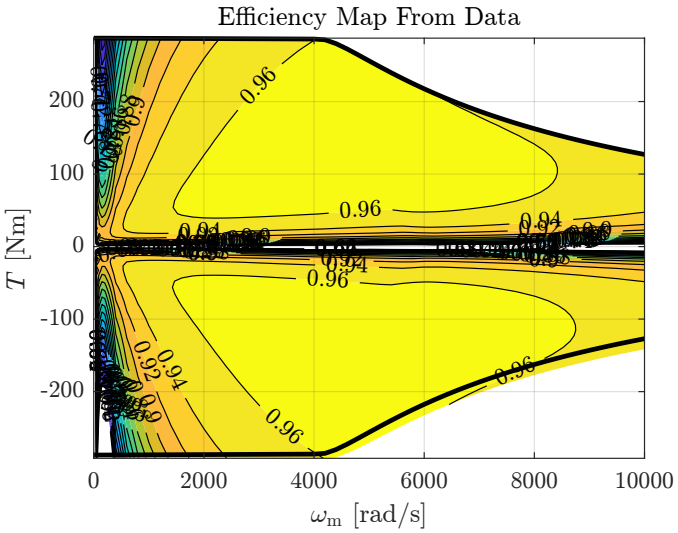

Fig. 3. Motor efficiency map resulting from real data.

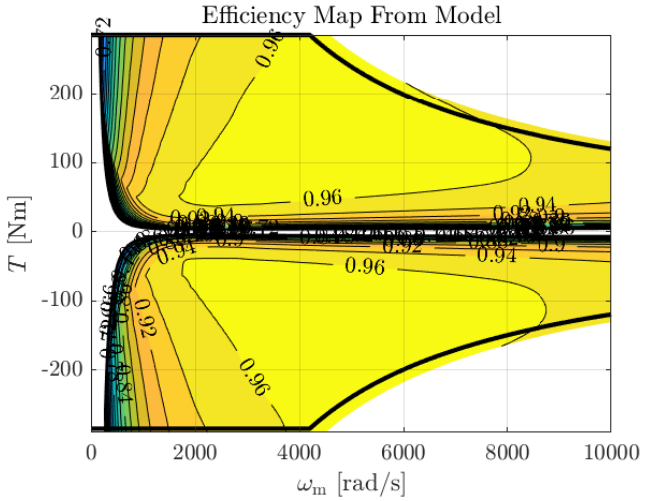

Fig. 4. Motor efficiency map resulting from model .

D. Energy-optimal Solution for the CVT

Instead of following previous methods such as that from [20], we develop a new method for finding the energy-optimal solution for the control of a CVT. This method is made possible by the quasi-static approach in combination with the motor model from Section II-C. The property of the motor model we leverage is the knowledge of the optimal operating point for each motor power P_{m}, this is the point where the power loss is the lowest. The idea becomes clearer if one looks at Fig. 2. There, the ω_{m} where $P_{\mathrm{m,loss}}$ is the lowest is clearly visible.

Since the variable that is interesting in the transmission operation is the gear ratio γ, the motor model (9) must be written in terms of γ.

$$P_{\mathrm{m,loss}} = \frac{d_0}{\gamma} + d_1 + d_2 \cdot \gamma, \tag{17}$$

where, for clarity, a new set of coefficients d_0, d_1 and d_2 is introduced that are related to the coefficients from (9) as $d_0 = \frac{p_0}{v/r_\text{w}}$, $d_1 = p_1$ and $d_2 = p_2 \cdot \frac{v}{r_\text{w}}$.

In order to find the point where $P_\text{m,loss}$ is lowest, the derivative of (17) has to be set equal to zero, yielding

$$d_2 \cdot \gamma^2 = d_0.$$

Only the solution in the positive domain has to be taken into account. The optimal operating point can now be written as

$$\gamma_\text{uc}^\star = \sqrt{\frac{d_0}{d_2}}, \tag{18}$$

where $\gamma_\text{uc}^\star$ is the gear that leads to the optimal operating speed of the motor. This way, the optimal unconstrained operating point is now known. However, the constraints still have to be applied.

Since (17) has a convex shape, the constrained optimum is the point that is closest to the unconstrained optimum whilst still satisfying the constraints. To find this point, the constraints (14), (15) and (16) can be rewritten in terms of γ as

$$\gamma \leq \omega_\text{m,max} \cdot \frac{r_\text{w}}{v}, \tag{19}$$

$$\gamma \geq \frac{|P_\text{m}|}{T_\text{m,max}} \cdot \frac{r_\text{w}}{v}, \tag{20}$$

and

$$\gamma \leq \frac{|P_\text{m}| - c_\text{m2}}{c_\text{m1}} \cdot \frac{r_\text{w}}{v}. \tag{21}$$

Since we impose no restrictions on the range of the gear ratios that can be selected, the constraint (5) for starting on a slope is not taken into account.

The minimal and maximal values that γ can take on can be determined by

$$\gamma_\text{max} = \min\left(\omega_\text{m,max} \cdot \frac{r_\text{w}}{v},\ \frac{|P_\text{m}| - c_\text{m2}}{c_\text{m1}} \cdot \frac{r_\text{w}}{v}\right) \tag{22}$$

and

$$\gamma_\text{min} = \frac{|P_\text{m}|}{T_\text{m,max}} \cdot \frac{r_\text{w}}{v}. \tag{23}$$

Now, the final step that has to be taken to find the constrained optimum for a CVT is to check $\gamma_\text{uc}^\star$ with the constraints in (22) and (23). Since (17) is convex, the constrained optimum $\gamma^\star$ can then be found as

$$\gamma^\star = \min(\gamma_\text{max}, \max(\gamma_\text{min}, \gamma_\text{uc}^\star)). \tag{24}$$

Thus, $\gamma^\star$ either takes the value of an active constraint or the value of $\gamma_\text{uc}^\star$. Note that all steps taken in this section apply to each individual time step of the drive cycle.

The instantaneous optimum method as applied here provides a path to find the optimal gear ratio for a CVT. The advantage over traditional convex optimization is that the problem can be solved entirely by matrix operations and is therefore extremely effective.

E. Energy-optimal Solution for the FGT

In order to find the optimal gear ratio for an FGT, the same method is used as in Section II-D, with the difference that now solely one optimal gear ratio has to be found. Hereto, we note that the coefficients can be summed whilst the model is still correct. This additive property of the model is used to find the optimal gear $\gamma^\star$. The total energy loss J is

$$J = \sum_{t=0}^{T} P_\text{m,loss}\, \Delta t. \tag{25}$$

Within the scope of this project, minimizing the energy loss J is equivalent to minimizing the sum of the power loss. Since in the case of an FGT, the gear ratio γ is constant, it can be extracted from (17). The sum of the power loss can then be written as

$$\sum_{t=0}^{T} P_\text{m,loss}\, \Delta t = \frac{e_0}{\gamma} + e_1 + e_2 \cdot \gamma\,, \tag{26}$$

where a new set of parameters is introduced for clarity. They relate to the constants in (17) as $e_0 = \sum_{t=0}^{T} d_0\, \Delta t$, $e_1 = \sum_{t=0}^{T} d_1\, \Delta t$ and $e_2 = \sum_{t=0}^{T} d_2\, \Delta t$. Now, the same steps as in Section II-D can be followed to arrive at the energy optimal gear ratio. First, the derivative of the power loss is set to zero. This results in

$$e_2 \cdot \gamma^2 = e_0.$$

The optimal unconstrained gear ratio can now be written as

$$\gamma_\text{uc}^\star = \sqrt{\frac{e_0}{e_2}}. \tag{27}$$

Since there is now one gear ratio to control the motor speed for the entire drive cycle, the constraints have to be adapted in order to apply to the FGT. Since (26) is convex, the constrained optimum is the point that is closest to the unconstrained optimum whilst still satisfying the constraints. In order to make sure the constraints are satisfied at each time step, the constraints (19), (20) and (21) are adapted to

$$\gamma \leq \min(\,\omega_\text{m,max} \cdot \frac{r_\text{w}}{v})\,, \tag{28}$$

$$\gamma \geq \max(\,\frac{|P_\text{m}|}{T_\text{m,max}} \cdot \frac{r_\text{w}}{v})\,, \tag{29}$$

and

$$\gamma \leq \min(\,\frac{|P_\text{m}| - c_\text{m2}}{c_\text{m1}} \cdot \frac{r_\text{w}}{v})\,, \tag{30}$$

where the max and min operators are necessary because P_m and v are vectors that depend on the drive cycle and vehicle model and the constraint has to be valid over the entire drive cycle. Furthermore, the constraint (5) has to be taken into account, it is therefore rewritten as

$$\gamma \geq \frac{m_\text{v} \cdot g \cdot \sin(\alpha_0) \cdot r_\text{w}}{T_\text{m,max} \cdot \eta_\text{fgt}}. \tag{31}$$

Constraints (22) and (23) can now be adapted to find the minimal and maximal values that γ can take on as

$$\gamma_{\text{max}} = \min\left(\min(\,\omega_{\text{m,max}} \cdot \frac{r_{\text{w}}}{v}),\ \min(\,\frac{|P_{\text{m}}| - c_{\text{m2}}}{c_{\text{m1}}} \cdot \frac{r_{\text{w}}}{v})\right) \tag{32}$$

and

$$\gamma_{\text{min}} = \max\left(\max(\frac{|P_{\text{m}}|}{T_{\text{m,max}}} \cdot \frac{r_{\text{w}}}{v}),\ \frac{m_{\text{v}} \cdot g \cdot \sin(\alpha_0) \cdot r_{\text{w}}}{T_{\text{m,max}} \cdot \eta_{\text{fgt}}}\right). \tag{33}$$

At this stage, the final step has to be taken again to check $\gamma^{\star}_{\text{uc}}$ with the constraints in (32) and (40). The constrained optimum $\gamma^{\star}$ can be found once more by applying (24) to make sure that $\gamma^{\star}$ either takes the value of an active constraint or the value of $\gamma^{\star}_{\text{uc}}$.

The instantaneous optimum method as applied here provides a way to find the optimal gear ratio for an FGT. This implementation of convex programming can be solved entirely by matrix operations and is therefore very effective.

F. Energy-optimal Solution for the MGT

To solve the combinatorial problem of optimizing the gear ratios and gear strategy for an MGT, a more involved method has to be employed than that of Section II-D and II-E. The method consists of two parts that work together in an iterative manner. The first part determines the optimal gear strategy. The second part determines the optimal gear ratios for a given gear strategy. This part is similar to the method described in Section II-E.

1) Determining the Optimal Gear Strategy for an MGT: A dynamic-programming based method is used to determine the optimal gear strategy for an MGT. For each gear that is available at a time step, the optimal next gear change is identified. This is done starting at the second to last time step and iterating backwards to the first time step.

First, the input power P_{dc} is calculated for each gear using the motor model (9). The calculation is done over the entire length of the drive cycle N. The result is a matrix P_{allgears} which has N rows, n_{gears} columns and holds the input power for each gear, where n_{gears} is the number of gears. A binary matrix I is determined of the same size as P_{allgears} which is 1 if the maximum power, torque or motor speed have been surpassed, and 0 otherwise. This matrix identifies the infeasible space.

Using these matrices, the cost of shifting to a different gear or staying at the same gear C_{next} can be calculated as

$$C_{\text{next},i,n} = P_{\text{allgears},n} + G_c \cdot C_{\text{param}} + I_n \cdot C_{\text{penalty}}, \tag{34}$$

where i is the current gear, n is the next gear, G_c is a binary vector that is 0 if $n = i$ and 1 otherwise, C_{param} is the cost for a gear change and C_{penalty} is a very large penalty function for entering the infeasible space. In the end C_{next} has the same number of rows and columns as the number of gears. Now, the optimal result for each current gear i is selected as

$$C_{\text{prev},i} = \min\left(C_{\text{next},i} + C_{\text{prev,i+1}}\right), \tag{35}$$

Algorithm 1 Dynamic Programming-Based Algorithm

```
j = N − 1
while j ≥ 1 do
    Find C_next,i,n according to (34)
    Find C_prev,i according to (35)
    Find γ_next corresponding with C_prev,i
    j = j − 1
Find γ_1 corresponding with min(C_prev,1)
j = 1
while j ≤ N − 1 do
    γ_j+1 = γ_next corresponding with γ_j
    j = j + 1
```

where C_{prev} is a vector with the same length as the number of gears which holds the result of previous iterations and $C_{\text{next},i}$ holds the cost of shifting to the next gear or staying in the current gear for the current iteration. By summing C_{prev} and C_{next} the total cost of switching to or staying in a certain gear is calculated for all future iterations from the current one. This way the total cost is summed and saved in $C_{\text{prev},i}$. A vector γ_{next} with the same width as the number of gears and the same length as the number of time steps is used to keep track of the optimal gear change. The values in γ_{next} indicate for each current gear, which is the optimal gear to switch to, or to stay in, before the next time step. Now, algorithm 1 can be executed to reach an optimal gear strategy.

2) Determing the Optimal Gear Ratios for an MGT: Once more, we leverage the additive property of the model to find the optimal gear ratio for each gear γ_i, where i ranges from 1 to the total number of gears n_{gears}.

Similar to the case of the FGT, the gear ratios can be extracted from (17) because they are constants. The total energy loss J can once more be determined by (25). A binary variable $b_i(t)$ is introduced where $b_i(t) = 1$ if $\gamma(t) = \gamma_i$. The sum of the power loss can then be written as

$$\sum_{t=0}^{T} P_{\text{m,loss}}\,\Delta t = \sum_{i=1}^{n_{\text{gears}}} \frac{f_{0,i}}{\gamma_i} + f_{1,i} + f_{2,i} \cdot \gamma_i, \tag{36}$$

where a new set of parameters is introduced for clarity's sake. The parameters $f_{0,i}$ - $f_{2,i}$ are derived from the constants in (17) as $f_{0,i} = \sum_{t=0}^{T} d_0 \cdot b_i\,\Delta t$, $f_{1,i} = \sum_{t=0}^{T} d_1 \cdot b_i\,\Delta t$ and $f_{2,i} = \sum_{t=0}^{T} d_2 \cdot b_i\,\Delta t$.

The optimal solution for (36) can be found by determining the optimal solutions for each individual gear. The derivatives for each gear ratio have to be set equal to zero, resulting in

$$f_{2,i} \cdot \gamma_i^2 = f_{0,i}.$$

The optimal unconstrained gear ratio can now be written as

$$\gamma^{\star}_{\text{uc,i}} = \sqrt{\frac{f_{0,i}}{f_{2,i}}}. \tag{37}$$

Similarly to Section II-E, the constraints have to be adapted to the situation with multiple gears. Once more we use the

Algorithm 2 Iterative Algorithm

$\gamma_i = \gamma_{i,\text{start}}$
$J_{\text{prev}} = 1$
$J = 0$
while $||J - J_{\text{prev}}|| \geq \epsilon$ **do**
  $J_{\text{prev}} = J$
  Find optimal gear strategy by executing algorithm 1
  Find $\gamma_i^\star$ according to the method in Section II-F2
  $\gamma_i = \gamma_i^\star$
  Find J according to (25) and (36)

property that (36) is convex. The constrained optimum for each gear is the point that is closest to the unconstrained optimum whilst satisfying the constraints. The same adaptations of (19), (20) and (21) are used as in Section II-E, meaning that (28), (29) and (30) can be applied here.

Now (32) and (40) have to be adapted in order to apply the constraints to the correct gear ratios. Since the constraints have to be applied only at the time steps where a particular gear is selected, we briefly introduce time dependency denoted by j. The minimal and maximal values that γ_i can attain can be written as

$$\gamma_{\text{max},i} = \min\left(\min(\,\omega_{\text{m,max}} \cdot \frac{r_\text{w}}{v_j}),\ \min(\,\frac{|P_\text{m}| - c_{\text{m2}}}{c_{\text{m1}}} \cdot \frac{r_\text{w}}{v_j})\right) \quad \forall j \in b_{i,j} = 1 \tag{38}$$

and

$$\gamma_{\text{min},i} = \max(\,\frac{|P_\text{m}|}{T_{\text{m,max}}} \cdot \frac{r_\text{w}}{v})\,\forall j \in b_{i,j} = 1. \tag{39}$$

For one of the gears, the slope start constraint (5) has to be applied. Hereto, (39) is adapted for γ_1 as

$$\gamma_{\text{min},1} = \max\left(\max(\frac{|P_\text{m}|}{T_{\text{m,max}}} \cdot \frac{r_\text{w}}{v_j}),\ (\frac{m_\text{v} \cdot g \cdot \sin(\alpha_0) \cdot r_\text{w}}{T_{\text{m,max}} \cdot \eta_{\text{mgt}}})\right) \quad \forall j \in b_{1,j} = 1. \tag{40}$$

Finally, the optimal gear ratios $\gamma_i^\star$ can be found by

$$\gamma_i^\star = \min(\gamma_{\text{max},i}, \max(\gamma_{\text{min},i}, \gamma_{\text{uc},i}^\star)). \tag{41}$$

3) Finding the Optimal Gear Strategy and Design: Now, the combinatorial problem of finding the optimal gear strategy and the optimal gear ratios can be solved by executing algorithm 2. The algorithm is terminated when the change in total energy loss J is smaller than a threshold value ϵ.

This iterative method provides local minima for the optimization of the gear ratios and gear strategy. However, there are no global optimality guarantees. Due to the speed of both the DP based method and the instantaneous optimum method, the algorithm should quickly converge.

G. Motor Sizing

The speed of the methods described in Sections II-D, II-E and II-F allow for a brute force approach to motor sizing. The motor will be scaled along a scaling parameter s where

$$s = \frac{P_{\text{m,max}}}{\overline{P}_{\text{m,max}}}. \tag{42}$$

The coefficients can then be scaled as

$$\begin{aligned} p_i &= s \cdot \overline{p}_i \ \ \forall i \in 0,1,2 \\ c_{\text{m},i} &= s \cdot \overline{c}_{\text{m},i} \ \ \forall i \in 0,1. \end{aligned} \tag{43}$$

This way, the motor is scaled linearly in the maximum power and the convexity of the model is preserved.

H. Energy-optimal Solution for the MGT via MIQP

We do not provide global optimality guarantees for the proposed iterative method to jointly optimize the design and operation of an MGT. Still, it would be insightful to benchmark the optimality of our solution with respect to the global optimum. To this end, one possibility would be to solve our problem with mixed-integer convex programming. However, given the mathematical structure of our problem (convex, but fractional and linear) there are no off-the-shelf optimization algorithms that could solve it in a mixed-integer framework. Specifically, it could not be even framed as a mixed-integer second-order conic program. Therefore, we consider a slightly less accurate version of the EM model and solve it both with our algorithm 2 and mixed-integer quadratic programming. The version of the EM model that is used is

$$P_{\text{m,loss}} = p_1 + p_2 \cdot \omega_\text{m} + p_3 \cdot \omega_\text{m}^2, \tag{44}$$

where p_1, p_2 and p_3 are determined in the same fashion as described in Section II-C.

The global optimum of joint optimization of the gear ratios and gear strategy can be found via MIQP by using the big-M method. A parameter M is introduced that is set to be a very large value, such as 10 times the total required power. The constraints (5), (14), (15) and (16) that represent the requirements on starting in a slope, the maximum motor speed, the maximum torque and the maximum power, respectively, are applied. The same b_i as in Section II-F is introduced, that is, 1 if a gear is engaged and 0 if a gear is disengaged. The constraint on the input power is relaxed to

$$P_\text{dc} \geq P_\text{m} + P_{\text{m,loss}}. \tag{45}$$

The relaxation can be effected because the relation will hold with equality if the total energy is minimized. The power loss $P_{\text{m,loss}}$ is determined by (44).

The motor speed ω_m is determined by

$$\omega_m \geq b_i \cdot \gamma_i \cdot \frac{v}{r_w} - b_i \cdot M \tag{46}$$

and

$$\omega_m \leq b_i \cdot \gamma_i \cdot \frac{v}{r_w} + b_i \cdot M. \tag{47}$$

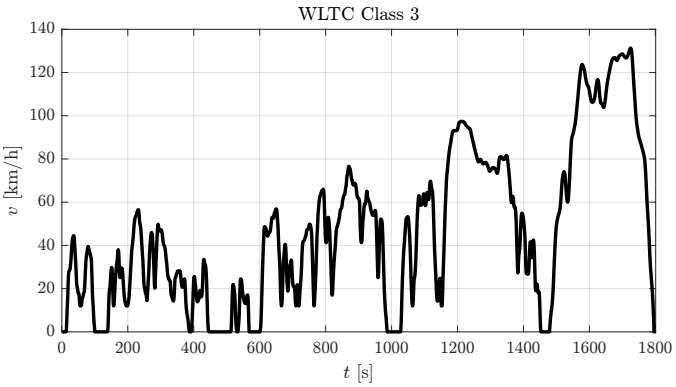

Fig. 5. Worldwide harmonized Light-duty vehicles Test Cycle, Class 3.

A constraint is added to make sure that one gear is selected at all times.

$$\sum_{i}^{n_{\text{gears}}} b_i = 1. \tag{48}$$

Finally, the objective function is chosen as the total energy that has to be put into the EM.

$$E = \sum_{0}^{T} P_{\text{dc}}\ \Delta t. \tag{49}$$

The optimization problem for both the gear ratios and the gear strategy can now be stated as:

Problem 1 (MIQP) *Given the electric vehicle architecture of Fig. 1 with a multiple-gear transmission, the optimal gear ratio and optimal gear strategy are the solution of*

$$\min_{x_p, x_c}\ E$$
$$\text{s.t. (5),(14),(15),(16),(44),(45),(46),(47),(48),(49)}$$

where the control parameters are $x_c = b_i$ and the sizing parameters are $x_p = \gamma_i$.

III. Results

In this section we present the results in the following order: First, the experimental design will be outlined in Section III-A. Second, we present the numerical results in Section III-B. Finally, the results will be validated using both nonlinear and convex methods in Section III-C.

A. Experimental Design

The vehicle will complete the Worldwide harmonized Light-duty vehicles Test Cycle (WLTC) Class 3. The speed profile of this drive cycle is shown in Fig. 5. The vehicle that is employed is a compact family car. The vehicle parameters that are used to obtain the numerical results are shown in Table I.

TABLE I
Vehicle Parameters.

Parameter	Symbol	Value	Unit
Vehicle base mass	m_0	1450	kg
CVT mass	m_{cvt}	80	kg
FGT and MGT base mass	$m_{\text{g},0}$	50	kg
added mass per gear	m_{gw}	5	kg/gear
CVT efficiency	η_{cvt}	0.96	-
FGT efficiency	η_{fgt}	0.98	-
MGT efficiency	η_{mgt}	0.98	-
Wheel radius	r_{w}	0.316	m
Air drag coefficient	c_{d}	0.29	-
Frontal area	A_{f}	0.725	m^2
Air density	ρ	1.25	kg/m^2
Rolling resistance coefficient	c_{r}	0.02	-
Gravitational constant	g	9.81	m/s^2
Minimal Slope	α_0	14	$^\circ$
Gearshift Cost	C_{param}	300	J
Threshold Parameter	ϵ	0.0001	%

TABLE II
Optimization Results.

Transmission	Total Energy	Energy Loss	Vehicle Mass	Max Power
FGT	9.281 MJ	804.5 kJ	1564 kg	65 kW
2-Speed MGT	8.967 MJ	548.8 kJ	1551 kg	45 kW
3-Speed MGT	8.961 MJ	520.6 kJ	1556 kg	45 kW
4-Speed MGT	8.972 MJ	510.0 kJ	1561 kg	45 kW
5-Speed MGT	8.988 MJ	503.5 kJ	1566 kg	45 kW
CVT	9.190 MJ	499.5 kJ	1572 kg	47 kW
2-Speed MGT w Shift-Cost	8.973 MJ	554.3 kJ	1551 kg	45 kW
3-Speed MGT w Shift-Cost	8.976 MJ	535.4 kJ	1556 kg	45 kW
4-Speed MGT w Shift-Cost	8.989 MJ	526.3 kJ	1561 kg	45 kW
5-Speed MGT w Shift-Cost	9.007 MJ	523.0 kJ	1566 kg	45 kW

B. Numerical Results

The problems from Sections II-D, II-E and II-F do not require programming solvers and can be solved by matrix operations only. The Dynamic programming-based algorithm 1 takes approximately 7 ms to run. The iterative algorithm 2 takes approximately 180 ms to run. Including brute forcing of the motor size, the algorithms take a few seconds to run. The longest run time in the case for a 5-speed transmission is 3.4 s.

The results of the algorithms from Sections II-D, II-E and II-F are shown in Table II. It is evident that the FGT yields the worst performance. The main reason for this is that, owing to the constraint for starting on a slope (5), the motor needs to be able to deliver a high torque and therefore adds mass. Furthermore, the increased size of the motor decreases the number of operating points that lie in the optimal efficiency region. The CVT is outperformed by every MGT. The added benefits of being able to vary the gear ratio do not compensate

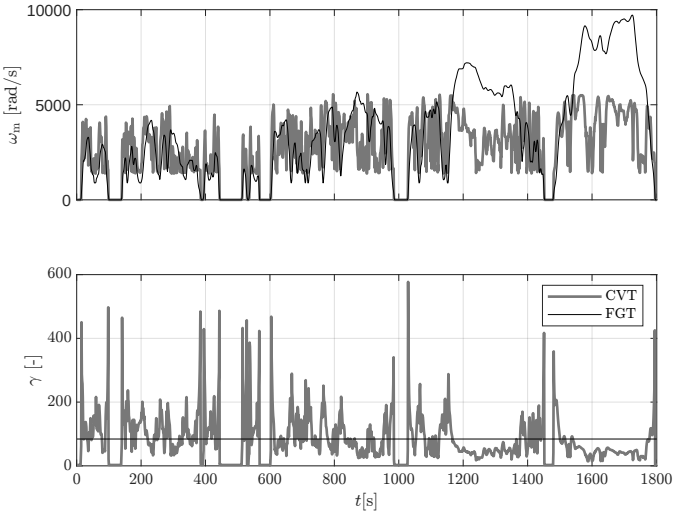

Fig. 6. Optimal motor speed and gear values for an FGT and a CVT.

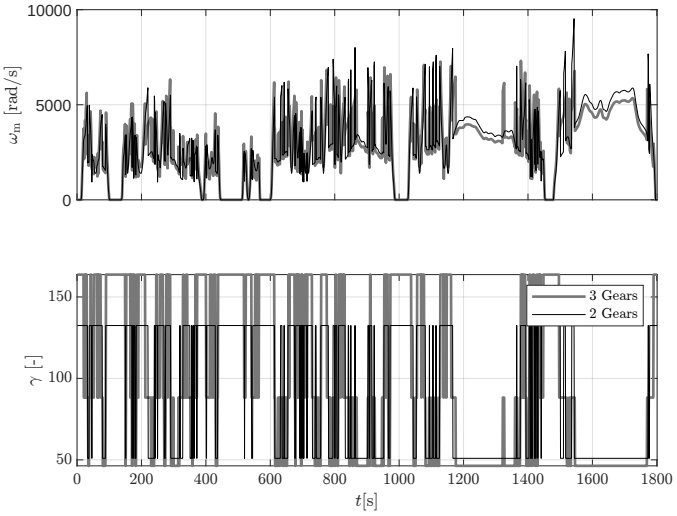

Fig. 7. Optimal motor speed and gear values for a 2 and a 3-speed MGT.

for the added weight and the reduced efficiency.

In Fig. 6 the motor speed and gear values resulting from the algorithms in Sections II-E and II-D for an FGT and a CVT are shown. The CVT is able to vary the gear ratios and therefore the motor speed is being kept much more constant.

It is interesting to note that the benefits of adding gear ratios has a point of diminishing returns. While the loss of energy goes down as the number of gears is increased, the increase in required energy due to increased mass causes a higher overall energy consumption. For 2 and 3 gear transmissions the increased possibilities of regulating the gear ratios lead to greater energy consumption. However, for 4 and 5 gear transmissions the increased variability in gear ratios does not overcome the added weight of more gears.

Fig. 7 and 8 showcase the motor speed and gear values resulting from the algorithm in Section II-F. From 2 to 4 gear transmissions, the increase in gears leads to a better management of the motor speed. In Fig. 8, the diminishing returns of an added gear become visible. The difference in the management of the motor speed becomes small for 4 and 5-speed transmissions.

The suppression of the number of gear changes via a gearshift cost means that the energy consumption of MGTs is increased. However, the MGTs still outperform the CVT and the FGT. The best performing transmission changes from the 3-speed MGT to the 2-speed MGT when the gearshift cost is applied. This is a result of the diminished benefit of gear changes. The motor speed and gear values for an MGT with gearshift cost is shown in Fig. 9 and 10. When compared to Fig. 7 and 8, the suppression of gear changes via the gearshift cost becomes clearly visible.

The operating points are plotted onto the motor map for an FGT, CVT and MGTs in Fig. 11, 12 and 13-16, respectively. Because of the increased size and lack of motor speed regulation, many operating points lie outside of the region where efficiency is best. In contrast, the CVT can manage the

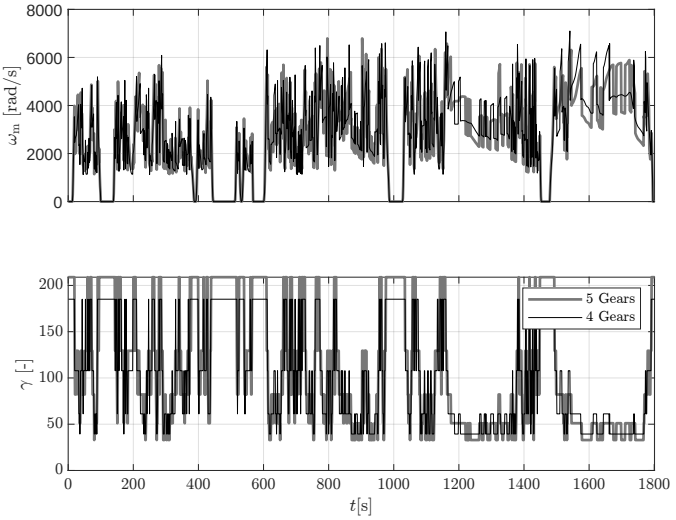

Fig. 8. Optimal motor speed and gear values for a 4 and a 5-speed MGT.

operating points very well. For the MGTs, the operating points come closer to the areas of high efficiency as the number of gears is increased.

C. Validation

To validate the results, three steps are taken. First, the globally optimal solutions resulting from problem 1 are obtained. Second, the methods of Sections II-D, II-E and II-F are applied to the quadratic motor model (44). Finally, in order to compare the results given by different motor models, the results obtained with both the fractional model (9) and the quadratic model (44) are simulated using the original nonlinear motor data. This three-step validation is done to compare the results from the methods of Sections II-D, II-E and II-F to the results of the MIQP of problem 1. However, since the MIQP requires a quadratic motor model, the results cannot be compared directly. By first showing the comparison between the MIQP of problem 1 and our methods applied

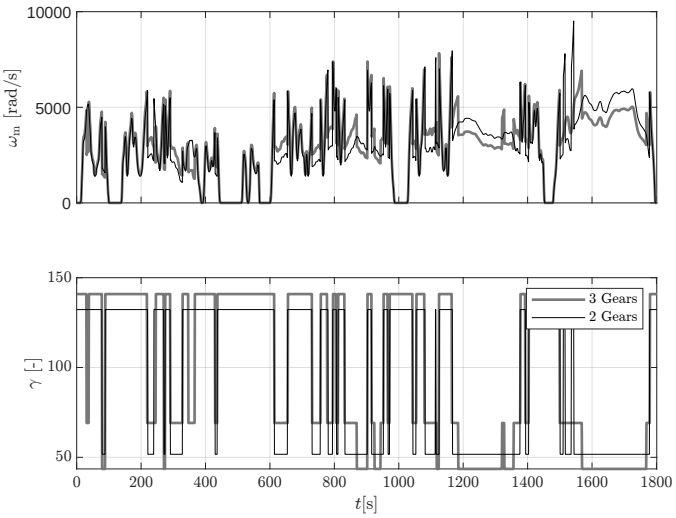

Fig. 9. Optimal motor speed and gear values for a 2 and a 3-speed MGT. Result with gearshift cost.

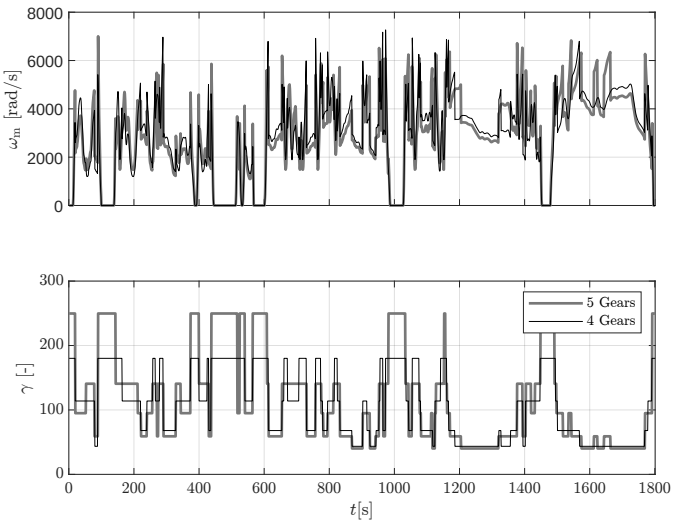

Fig. 10. Optimal motor speed and gear values for a 4 and a 5-speed MGT. Result with gearshift cost.

with a quadratic motor model and then comparing those results to those obtained with our model, a thorough validation procedure is applied. The results of the validation procedure are shown in Table III.

First, we compare results obtained by solving the MIQP with results obtained by applying the methods in Sections II-E and II-F on the quadratic EM model (44). For the FGT, the gear ratio obtained with the MIQP and the gear ratio obtained with the method in Section II-E applied on the quadratic model are identical. The gear ratios obtained with the MIQP for a 2-speed MGT are $\gamma_1 = 61.4169$ and $\gamma_2 = 157.3059$. The gear ratios obtained with the method in Section II-F applied on the quadratic model for a 2-speed MGT are $\gamma_1 = 61.4152$ and $\gamma_2 = 152.8208$. The resulting total energy obtained with the MIQP and the method of Section II-E differs less than 0.03%, with the very slight advantage going to the method of

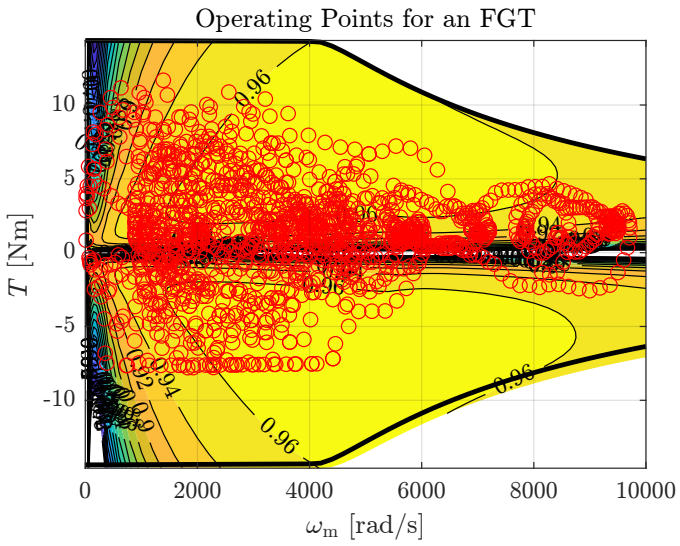

Fig. 11. The resulting operating points for the FGT. The result is plotted over the scaled original motor map.

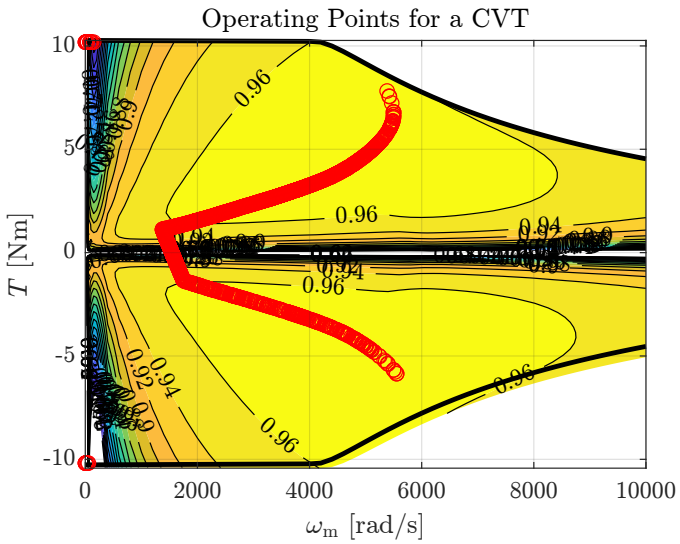

Fig. 12. The resulting operating points for the CVT. The result is plotted over the scaled original motor map.

TABLE III
VALIDATION RESULTS.

Transmission	**Total Energy Fractional Model**	**Total Energy Simulation Fractional Model**	**Total Energy Simulation Quadratic Model**	**Total Energy Quadratic Model**
FGT	9.281 MJ	9.239 MJ	9.241 MJ	9.312 MJ
2-Speed MGT	8.967 MJ	8.954 MJ	8.974 MJ	9.019 MJ
3-Speed MGT	8.961 MJ	8.955 MJ	8.983 MJ	9.014 MJ
4-Speed MGT	8.972 MJ	8.970 MJ	9.003 MJ	9.026 MJ
5-Speed MGT	8.988 MJ	8.985 MJ	9.025 MJ	9.044 MJ
CVT	9.190 MJ	9.197 MJ	9.243 MJ	9.249 MJ

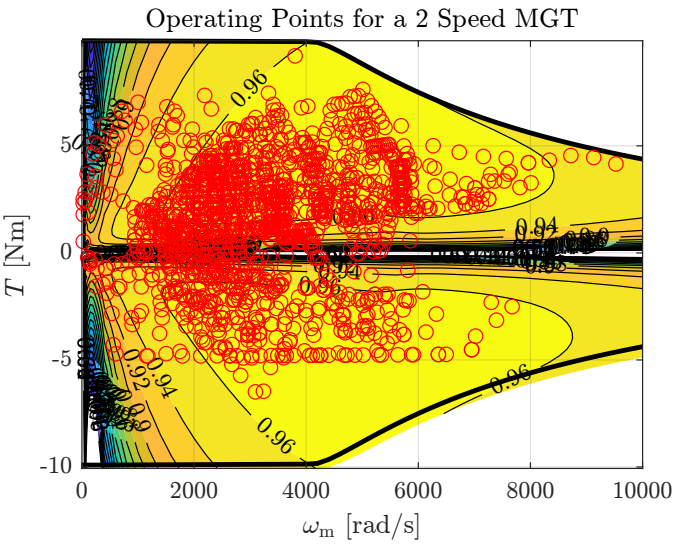

Fig. 13. The resulting operating points for the 2-speed MGT. The result is plotted over the scaled original motor map.

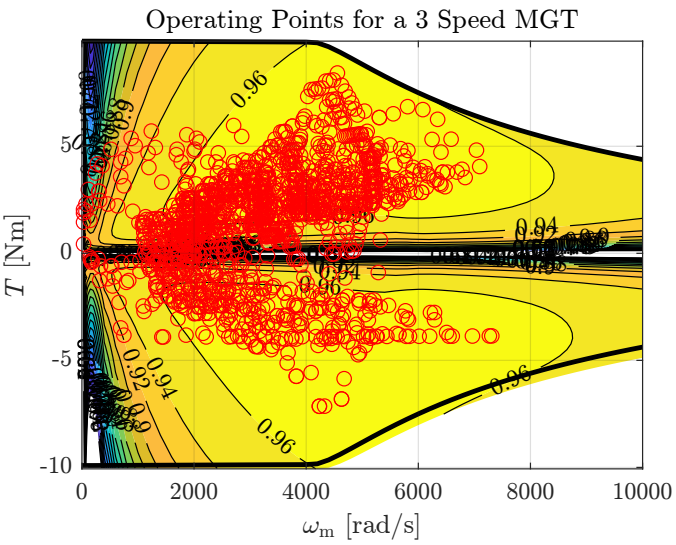

Fig. 14. The resulting operating points for the 3-speed MGT. The result is plotted over the scaled original motor map.

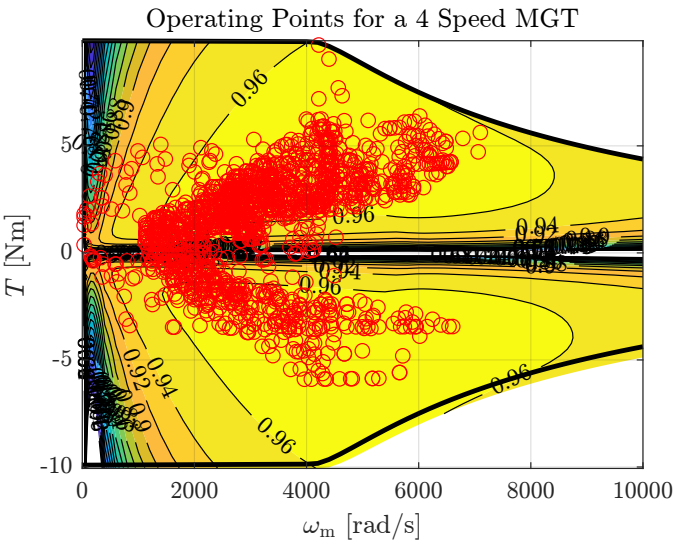

Fig. 15. The resulting operating points for the 4-speed MGT. The result is plotted over the scaled original motor map.

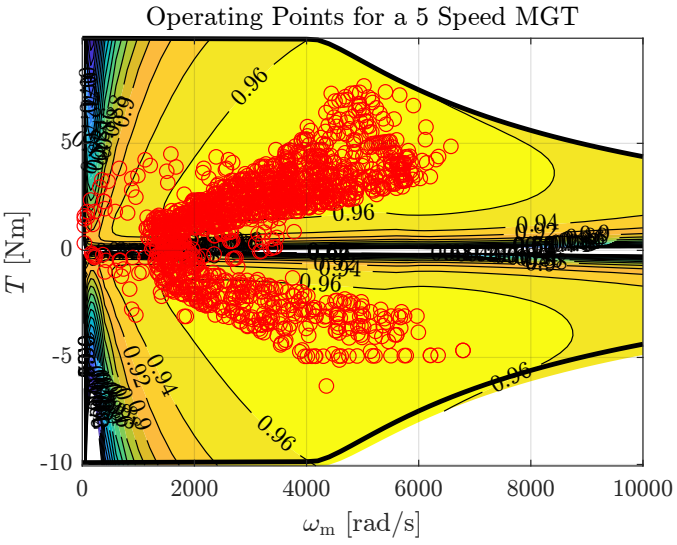

Fig. 16. The resulting operating points for the 5-speed MGT. The result is plotted over the scaled original motor map.

Section II-E. A possible explanation for the difference is the cutoff threshold of the solver for the MIQP. When nonlinear simulation is applied to the results of te MIQP and the method of Section II-E, the difference in total energy is less than 0.003%.

Second, we simulate the results obtained with the fractional model (9) and the methods of Sections II-D, II-E and II-F. When the simulation results obtained with the fractional model (9) are compared to the simulation results obtained with the quadratic model (44) in terms of total energy, the quadratic model is outperformed every time. Interestingly, the fractional model and the quadratic model result in the same EM sizes.

Finally, the result of the simulation of gear ratios and strategies obtained with the fractional model (9) is compared to the result of the fractional model. Whilst a similar trend is noticeable, the simulation results show that the 2-speed MGT outperforms the 3-speed MGT. The model results indicate that this is the other way around. The results are close in both cases and the difference is likely caused by modeling inaccuracies.

IV. Conclusions

In this thesis we explored the possibility of jointly optimizing the design and control of a battery electric vehicle transmission. Furthermore, the sizing of the electric motor was included in the optimization. To this end, we introduced methods leveraging both convex programming and dynamic programming that require little computation time. We applied our methods to a compact family car with multiple transmission types. Our modeling approach was validated with

nonlinear simulations showing high agreement, whilst the optimal solution found for a multiple gear transmission by our algorithm was found to be in line with the global optimum computed via mixed-integer quadratic programming. Our results show that by using a 2-speed transmission, the energy consumption of a battery electric vehicle can be reduced by 3% and 2.5% compared to a fixed-gear transmission and a continuously variable transmission, respectively.

This work opens the field for several extensions. First, the relatively high fidelity of the proposed convex models could be leveraged for more general powertrain control and optimization problems. Second, the methods can be used with a multitude of different motor models. Furthermore, the methods do not strictly apply to a compact family vehicle. Multiple topologies can be examined, including both light-vehicles and heavy-duty vehicles.

ACKNOWLEDGMENT

The author would like to thank Dr. Ir. Mauro Salazar for his excellent guidance and constructive criticism. The author would also like to thank Olaf Korzilius for the many fruitful discussions as well as Dr. Ilse New for proofreading this thesis.

REFERENCES

[1] F. Un-Noor, S. Padmanaban, L. Mihet-Popa, M. Mollah, and E. Hossain, "A Comprehensive Study of Key Electric Vehicle (EV) Components, Technologies, Challenges, Impacts, and Future Direction of Development," *Energies*, vol. 10, no. 1217, 2017.

[2] I. (2020), "Global EV outlook 2020, IEA, Paris," https://www.iea.org/reports/global-ev-outlook-2020, accessed: 2020-07-15.

[3] J. Y. Yong, V. K. Ramachandaramurthy, K. M. Tan, and N. Mithulananthan, "A review on the state-of-the-art technologies of electric vehicle, its impacts and prospects," *Renewable and Sustainable Energy Reviews*, vol. 49, pp. 365–385, 2015.

[4] T. Franke, M. Günther, M. Trantow, and J. Krems, "Does this range suit me? range satisfaction of battery electric vehicle users," *Applied Ergonomics*, vol. 65, pp. 191–199, 2017.

[5] O. Egbue and S. Long, "Barriers to widespread adoption of electric vehicles: An analysis of consumer attitudes and perceptions," *Energy Policy*, vol. 48, pp. 717–729, 2012.

[6] S. Ebbesen, P. Elbert, and L. Guzzella, "Engine downsizing and electric hybridization under consideration of cost and drivability," *Oil Gas Science and Technology*, vol. 68, no. 1, pp. 109–116, 2013.

[7] V. Saini, S. Singh, S. NV, and H. Jain, "Genetic Algorithm Based Gear Shift Optimization for Electric Vehicles," *SAE International Journal of Alternative Powertrains*, vol. 5, no. 2, pp. 348–356, 2016.

[8] J. Ritzmann, A. Christon, M. Salazar, and C. Onder, "Fuel-optimal power split and gear selection strategies for a hybrid electric vehicle," in *International Conference on Engines Vehicles*, ser. SAE Technical Papers. Society of Automotive Engineers (SAE), 2019.

[9] V. Ngo, T. Hofman, M. Steinbuch, and A. Serrarens, "Optimal control of the gearshift command for hybrid electric vehicles," *IEEE Transactions on Vehicular Technology*, vol. 61, no. 8, pp. 3531–3543, 2012.

[10] T. Nüesch, P. Elbert, M. Flankl, C. Onder, and L. Guzzella, "Convex Optimization for the Energy Management of Hybrid Electric Vehicles Considering Engine Start and Gearshift Costs," *Energies*, vol. 7, no. 2, pp. 834–856, 2014.

[11] N. Robuschi, M. Salazar, N. Viscera, F. Braghin, and C. H. Onder, "Minimum-fuel Energy Management of a Hybrid Electric Vehicle via Iterative Linear Programming," *IEEE Transactions on Vehicular Technology*, Submitted 2020.

[12] N. Murgovski, L. Johannesson, H. Xiaosong, B. Egardt, and J. Sjöberg, "Convex relaxations in the optimal control of electrified vehicles," *American Control Conference,*, 2015.

[13] N. Murgovski, L. Johannesson, J. Sjöberg, and B. Egardt, "Component sizing of a plug-in hybrid electric powertrain via convex optimization," *Mechatronics*, vol. 22, pp. 106–120, 2012.

[14] T. Hofman and N. H. J. Janssen, "Integrated design optimization of the transmission system and vehicle control for electric vehicles," *IFAC World Congress,*, 2017.

[15] P. Leise, L. C. Altherr, N. Simon, and P. F. Pelz, "Finding Global-Optimal Gearbox Designs for Battery Electric Vehicles," in *Advances in Intelligent Systems and Computing*, H. Le Thi, H. Le, and T. Pham Dinh, Eds. Springer Verlag, 2019, vol. 991, pp. 916–925.

[16] A. Sorniotti, S. Subramanyan, A. Turner, C. Cavallino, F. Viotto, and S. Bertolotto, "Selection of the Optimal Gearbox Layout for an Electric Vehicle," *SAE International Journal of Engines*, vol. 4, no. 1, pp. 1267–1280, 2011.

[17] B. Gao, Q. Liang, Y. Xiang, L. Guo, and H. Chen, "Gear ratio optimization and shift control of 2-speed I-AMT in electric vehicle," *Mechanical Systems and Signal Processing*, vol. 50-51, pp. 615–631, 2015.

[18] A. Morozov, K. Humphries, T. Rahman, T. Zou, and J. Angeles, "Drivetrain analysis and optimization of a two-speed class-4 electric delivery truck," *SAE Technical Paper*, 2019.

[19] O. Borsboom, C. Fahdzyana, M. Salazar, and T. Hofman, "Time-optimal control strategies for electric race cars with different transmission technologies," in *IEEE Vehicle Propulsion and Power Conference*, accepted 2020.

[20] F. Verbruggen, M. Salazar, M. Pavone, and T. Hofman, "Joint design and control of electric vehicle propulsion systems," in *European Control Conference 2020*, 2020.

[21] L. Guzzella and A. Sciarretta, *Vehicle propulsion systems*. Springer-Verlag Berlin Heidelberg, 2013.

APPENDIX A

TU/e Technische Universiteit Eindhoven University of Technology

Declaration concerning the TU/e Code of Scientific Conduct for the Master's thesis

I have read the TU/e Code of Scientific Conduct[i].

I hereby declare that my Master's thesis has been carried out in accordance with the rules of the TU/e Code of Scientific Conduct

Date

12-04-2021

Name

Jurjaan van der Hurk

ID-number

0907074

Signature

Submit the signed declaration to the student administration of your department.

[i] See: http://www.tue.nl/en/university/about-the-university/integrity/scientific-integrity/
The Netherlands Code of Conduct for Academic Practice of the VSNU can be found here also.
More information about scientific integrity is published on the websites of TU/e and VSNU

January 15 2016